HHS Public Access

Author manuscript

Mov Disord. Author manuscript; available in PMC 2020 March 01.

Published in final edited form as:

Mov Disord. 2019 March ; 34(3): 416–419. doi:10.1002/mds.27608.

Reproducible detection of nigral iron deposition in two Parkinson's disease cohorts

Jason Langley, PhD[1,+], **Naying He, MD, PhD**[2,+], **Daniel E. Huddleston, MD**[3,+], **Shengdi Chen, MD, PhD**[4], **Fuhua Yan, MD, PhD**[2], **Bruce Crosson, PhD**[3,6,7], **Stewart Factor, DO**[3], and **Xiaoping Hu, PhD**[1,5,*]

[1]Center for Advanced Neuroimaging, University of California, Riverside, Riverside, CA

[2]Department of Radiology, Ruijin Hospital, Shanghai Jiao Tong University School of Medicine, Shanghai, China

[3]Department of Neurology, Emory University, Atlanta, GA

[4]Department of Neurology and Institute of Neurology, Ruijin Hospital, Shanghai Jiao Tong University School of Medicine, Shanghai, China

[5]Department of Bioengineering, University of California, Riverside, Riverside, CA

[6]Department of Veterans Affairs Center for Visual and Neurocognitive Rehabilitation, Atlanta Veterans Affairs Medical Center, Decatur, GA, USA

[7]Department of Psychology, Georgia State University, Atlanta, GA, USA

Abstract

Background—Previous studies investigating nigral iron accumulation used T_2 or T_2*-weighted contrasts to define the ROIs in the substantia nigra with mixed results. Since these contrasts are not sensitive to neuromelanin, ROIs may have inadvertently missed SNpc. An approach sensitive to neuromelanin should yield consistent results. We examine iron deposition in ROIs derived from neuromelanin-sensitive and T_2*-weighted contrasts, respectively.

Methods—T_1-weighted and multi-echo gradient echo imaging data were obtained in two cohorts. Multi-echo gradient echo imaging data were analyzed using neuromelanin-sensitive SNpc ROIs as well as T_2*-weighted SNr ROIs.

*Correspondence to Xiaoping P. Hu, Ph.D., Provost Fellow, Professor and Chair Department of Bioengineering, University of California, Riverside, Materials Science and Engineering 205, Phone: (951) 827-2925, Fax: (951) 827-6416, xhu@engr.ucr.edu.
+These authors made equal contributions

Authors Roles

1) Research project: A. Conception, B. Organization, C. Execution; 2) Statistical Analysis: A. Design, B. Execution, C. Review and Critique; 3) Manuscript: A. Writing of the first draft, B. Review and Critique.

J.L.: 1A, 1B, 1C, 2A, 2B, 3A, 3B
N.H.: 1A, 1B, 1C, 2A, 2B, 3A, 3B
D.H.: 1A, 1B, 1C, 2B, 2C, 3A, 3B
S.C.: 1C, 2C, 3B
F.Y.:1C, 2C, 3B
S.F. 1A, 1C, 2C, 3B
X.H: 1A, 1C, 2C, 3B

Results—Compared with control subjects, significantly larger R_2* values were seen in SNpc of PD patients in both. Mean R_2* values in SNr of PD patients showed no consistency with one cohort showing a small statistically significant increase while the other cohort exhibited no statistical difference.

Conclusion—Mean R_2* in the SNpc defined by neuromelanin-sensitive MRI is significantly increased in PD.

Keywords

Parkinson's disease; substantia nigra pars compacta; iron; MRI; neuromelanin

Introduction

Prior to and following the onset of Parkinson's Disease (PD) symptoms, there is a progressive loss of melanized neurons in the substantia nigra (SN), a paired midbrain structure located near the red nucleus. SN is comprised of SN pars reticulata (SNr) and the SN pars compacta (SNpc) [1]. In healthy subjects, SNpc contains a dense distribution of neuromelanin containing dopaminergic neurons, and at the time of PD symptom onset, a significant portion of melaninzed neurons in SNpc have been lost [2,3]. Iron deposition occurs in SN concurrent with this loss [4].

MRI techniques, such as transverse relaxation rate (R_2 or R_2*) mapping have been applied to investigate PD-related iron deposition in SN [5–18]. However, no clear consensus in regard to iron deposition, as measured with iron sensitive MRI techniques, has emerged in the literature [19–21]. Increases in transverse relaxation rate [5–12,22] in the SN of PD patients have been reported but other studies have observed no differences in SN transverse relaxation rates [13–18]. This lack of consistency may be due small sample size or placement of SN regions of interest (ROIs). In the aforementioned studies, SN ROIs were defined in T_2-weighted images in the hypointense region between the cerebral peduncle and red nucleus. It is important to note that T_2/T_2*-weighted images not sensitive to neuromelanin and localization of SNpc is difficult in these images [23].

Neuromelanin-sensitive MRI (NM-MRI) generates contrast sensitive to neuromelanin (NM) [24–27] and SN seen in T_2/T_2*-weighted contrasts is spatially incongruent to the NM-MRI SN [28]. Thus, prior attempts to estimate iron deposition from PD using ROIs placed in T_2/T_2*-weighted images may not have been placed in the neuromelanin-rich areas that deteriorate in PD. This lack of robustness in identifying the PD-relevant portions of the SN could explain the variability in findings based on ROIs defined using T_2/T_2*-weighted images in previous studies examining PD-related iron deposition. In this work, we examine the reproducibility of PD effects on R_2* in the NM-MRI defined SNpc as well as SNr, defined in T_2*-weighted images, in different populations.

Materials and Methods

All subjects participating in the study gave informed written consent in accordance with protocols approved by the local institutional review boards. Data from two hospitals were

analyzed in this study. Data from Cohort 1, consisting of 69 subjects (37 PD and 32 control), were collected at the Emory Movement Disorders Clinic. Cohort 2 consisted of 91 subjects (43 PD and 48 control) and data were collected at Ruijin Hospital. PD subjects were recruited from local movement disorders clinics, and all PD subjects were clinically diagnosed with PD according to the UK Brain Bank criteria [29]. Control subjects at Emory University were recruited from the Emory Alzheimer's Disease Research Center normal population. Control individuals at Ruijin Hospital were recruited from the general population. Control participants were excluded from the study if they exhibited: 1) symptoms or signs of secondary or atypical parkinsonism [30]; 2) cognitive abnormalities i.e. had Montreal Cognitive Assessment (MOCA) score of less than 26 at Emory University Hospital or Mini-Mental State Examination (MMSE) score of less than 24 at Ruijin Hospital; 3) a history of territorial ischemic stroke or hemorrhagic stroke, epilepsy, brain tumor, multiple sclerosis, neurodegenerative disease, hydrocephalus, bipolar disorder or schizophrenia; 4) treatment with an antipsychotic or any other dopamine-blocking drug; or 5) any contraindications to MRI imaging.

Demographic information, including gender, age and years of education, was collected for each participant (Table 1). Severity of Parkinsonian symptoms were assessed in PD and control groups using the Unified Parkinsonian Disease Rating Scale (UPDRS)-III motor examination. For each cohort, patients were assessed and underwent imaging in the ON medication state.

Image Acquisition

Data from the first cohort were acquired on a 3 T MRI scanner (Prisma Fit, Siemens Medical Solutions, Malvern, PA) using a 64-channel receive only coil. Images from a MP-RAGE sequence (echo time (TE)/repetition time (TR)/inversion time=3.02/2600/800 ms, flip angle (FA)=8°, voxel size=0.8×0.8×0.8 mm^3) were used for registration from subject space to common space. T_2*-weighted data were collected with a 6 echo 3D gradient recalled echo (GRE) sequence: $TE_1/\Delta TE/TR$=4.92/4.92/50 ms, FOV=220×220 mm^2, matrix size of 448×336×80, in-plane resolution = 0.49×0.49 mm^2, slice thickness=1 mm, and GRAPPA acceleration factor=2.

Data from the second cohort were acquired on a GE 3 T MRI scanner (Signa HDxT, GE Medical Systems, Milwaukee, WI) using an 8 channel receive only coil. T_1-weighted structural images were acquired using a 3D fast SPGR sequence with the following parameters: TR/TE=5.529/1.724 ms, acquisition slices=196, matrix=256×256, FOV=256 mm, flip angle=12°, and slice thickness=1 mm. T_2*-weighted data were collected with a sixteen echo GRE 3D sequence: $TE_1/\Delta TE/TR$=2.7/2.9/59.3 ms, FA=12°, FOV=220×220 mm^2, matrix size=128×128×56, 1.72×1.72 mm^2 in-plane resolution, slice thickness=1 mm, and ASSET acceleration factor=2.

Substantia Nigra Atlases

Standard space T_2*-weighted hypointense SN (SNr) and SNpc neuromelanin atlases from [31] were used in this study. They were transformed to T_2*-weighted images using a process

similar to those outlined in [31,32]. A comparison of the spatial position of the two SN ROIs is shown in Figure 1.

R_2* calculation

R_2* values were estimated using a custom script in MATLAB by fitting a monoexponential model to the GRE images.

$$S_i = S_0 \exp\left(-R_2^* TE\right) \quad [1]$$

where S_0 denotes a fitting constant and S_i denotes the signal of a voxel at the ith echo time. Mean R_2* was measured in the SNpc mask as well in the T_2-weighted hypointense SNr mask.

Statistical Analysis

All statistical analyses were performed using IBM SPSS Statistics version 24 (IBM Corporation, Somers, NY, USA). Results are reported as mean±standard deviation. Group R_2* comparisons between PD patients and controls were made using a one tailed t-test. A p-value of 0.05 was considered significant for all statistical tests performed in this work. Receiver operator characteristic (ROC) curves were obtained for SNpc and SNr R_2* values.

Results

Mean R_2* values in SNpc, as defined by neuromelanin-sensitive MRI, were increased in the PD group of both cohorts. For cohort 1, mean SNpc R_2* values were 32.5 s^{-1} ± 5.6 s^{-1} and 27.5 s^{-1}±4.3 s^{-1} ($p<10^{-4}$) for PD and control groups, respectively. For the second cohort, mean SNpc R_2* values were 34.3 s^{-1}±4.9 s^{-1} and 29.5 s^{-1}±4.4 s^{-1} ($p=7\times10^{-4}$) for PD and control groups, respectively. Interestingly, conflicting results were observed in mean R_2* values in SNr ROIs derived from the T_2-weighted images showed elevated iron levels in the PD group of cohort 1 (PD: 37.8 s^{-1}±5.4 s^{-1}; control: 35.4 s^{-1}±5.2 s^{-1}; p=0.03), but not in the second cohort (PD: 40.7 s^{-1} ± 6.0 s^{-1}; control: 39.2 s^{-1}±8.4 s^{-1}; p=0.15). These results are summarized in Figure 2.

Mean SNpc R_2* outperformed mean SNr R_2* as a diagnostic biomarker in both cohorts. The area under the ROC curve (AUC) for mean SNpc R_2* in cohort 1 was 0.730 (standard error (SE)=0.082; 95% confidence interval (CI): 0.613–0.842; p=0.001). The AUC for mean SNr R_2* in cohort 1 was 0.604 (SE=0.067; 95% CI: 0.472–0.735; p=0.131). In cohort 2, the AUC for mean SNpc R_2* was 0.751 (SE=0.055; 95% CI: 0.643–0.860; $p<10^{-3}$), while the AUC for mean SNr R_2* was 0.461 (SE=0.055; 95% CI: 0.332–0.590; p=0.552). ROC curves are shown in Figure 2.

Discussion

The establishment of a reliable neuroimaging biomarker for assessing iron deposition in SN is necessary to assist in the development of disease modifying therapies and to track disease progression. Here, we found the mean R_2* in a standard space SNpc ROI derived from NM-

MRI images to be a reproducible biomarker in two separate cohorts. Further supporting the generalizability of these results, these cohorts were drawn from different populations, in the United States and China, respectively. These results suggest that mean SNpc R_2* may be a reliable neuroimaging biomarker for assessing PD-related iron deposition.

In contrast, mean R_2^* in the SNr ROI, as defined in T_2-weighted images, was found to be an inconsistent biomarker with cohort 1 showing a statistically significant difference between groups and cohort 2 not exhibiting a statistically significant difference between groups. This inconsistency in observing PD-related iron deposition using T_2-weighted images to define SN ROIs is in accordance with prior work [5–18]. The inconsistency of iron deposition present in prior studies may be at least partially explained by insensitivity of T_2- and T_2*-weighted images to neuromelanin [33] and to differences in ROIs used for SNpc and SNr in evaluating PD-related SN iron deposition [6,10,34]. In most of the previous studies, the SN ROI was defined to be the hypointense region between the red nucleus and cerebral peduncle in T_2/T_2*-weighted images. As NM-MRI signal colocalizes with neuromelanin [35] and nigral neuromelanin is present exclusively in the SNpc [2], these previous ROIs resided mostly in SNr, as opposed to SNpc, which is the critical structure for PD [36].

A biological rationale for the conflicting results observed in mean SNr R_2* values of the two cohorts examined in this study may be attributed to the spatial locations T_2*-weighted (i.e. SNr) and NM-MRI (i.e. SNpc) SN volumes. Prior work has found a non-zero overlap between the T_2*-weighted (i.e. SNr) and NM-MRI (i.e. SNpc) SN volumes [28]. In some subjects, iron deposition may be so pronounced in this region that it effectively skews R_2* in the rest of the T_2*-weighted SN ROI (i.e. SNr). In this case, a few subjects exhibiting this trait may induce statistically significant changes in studies with small populations.

As reported in histology [2,3], much of the degeneration in SN occurs inferior to the red nucleus. In imaging studies, this degeneration occurs in the superior and lateral-ventral portions of SNpc [37]. Some studies using T_2/T_2*-weighted images to define SN ROIs have placed these ROIs regions of SNc experiencing iron deposition and found increases in free water [38,39]. Studies using T_2/T_2*-weighted should choose ROIs in the inferior and posterior portions of the SN in T_2/T_2*-weighted images, or define SNc ROIs from NM-MRI [24–27] or multi-spectral MRI [40].

Conclusion

In summary, this study shows SNpc, as defined by NM-MRI, is sensitive to PD-related iron deposition with reproducible increased R_2*. In contrast, mean SNr R_2*, ascertain on an ROI defined using T_2*-weighted imaging, was found to be an inconsistent biomarker.

Acknowledgments

Funding Sources:

Xiaoping Hu, Jason Langley, and Daniel Huddleston receive funding from the Michael J. Fox Foundation (MJF 10854). Recruitment of control individuals for this research was facilitated by the Emory Alzheimer's Disease Research Center (NIH-NINDS P50-AG025688). The Emory MRI facility used in this study is supported in part by funding from a Shared Instrumentation Grant (S10) grant 1S10OD016413–01 to the Emory University Center for Systems Imaging Core. Fuhua Yan and Naying He receive funding from the Science and Technology Commission

of Shanghai Municipality (17411952700). Naying He receives funding from the Shanghai Sailing Program (18YF1414700).

Funding Disclosures

Nothing additional to report

References

1. Poewe W, Seppi K, Tanner CM, Halliday GM, Brundin P, Volkmann J, Schrag AE, Lang AE (2017) Parkinson disease. Nat Rev Dis Primers 3:17013. [PubMed: 28332488]
2. Fearnley JM, Lees AJ (1991) Ageing and Parkinson's disease: substantia nigra regional selectivity. Brain 114 (Pt 5):2283–2301. [PubMed: 1933245]
3. Damier P, Hirsch EC, Agid Y, Graybiel AM (1999) The substantia nigra of the human brain. II. Patterns of loss of dopamine-containing neurons in Parkinson's disease. Brain 122 (Pt 8):1437–1448. [PubMed: 10430830]
4. Wypijewska A, Galazka-Friedman J, Bauminger ER, Wszolek ZK, Schweitzer KJ, Dickson DW, Jaklewicz A, Elbaum D, Friedman A (2010) Iron and reactive oxygen species activity in parkinsonian substantia nigra. Parkinsonism Relat Disord 16 (5):329–333. [PubMed: 20219408]
5. Baudrexel S, Nurnberger L, Rub U, Seifried C, Klein JC, Deller T, Steinmetz H, Deichmann R, Hilker R (2010) Quantitative mapping of T1 and T2* discloses nigral and brainstem pathology in early Parkinson's disease. NeuroImage 51 (2):512–520. [PubMed: 20211271]
6. Du G, Lewis MM, Styner M, Shaffer ML, Sen S, Yang QX, Huang X (2011) Combined R2* and diffusion tensor imaging changes in the substantia nigra in Parkinson's disease. Mov Disord 26 (9): 1627–1632. [PubMed: 21618607]
7. Gorell JM, Ordidge RJ, Brown GG, Deniau JC, Buderer NM, Helpern JA (1995) Increased iron-related MRI contrast in the substantia nigra in Parkinson's disease. Neurology 45 (6):1138–1143. [PubMed: 7783878]
8. Graham JM, Paley MN, Grunewald RA, Hoggard N, Griffiths PD (2000) Brain iron deposition in Parkinson's disease imaged using the PRIME magnetic resonance sequence. Brain 123 Pt 12:2423–2431. [PubMed: 11099445]
9. Kosta P, Argyropoulou MI, Markoula S, Konitsiotis S (2006) MRI evaluation of the basal ganglia size and iron content in patients with Parkinson's disease. J Neurol 253 (1):26–32. [PubMed: 15981079]
10. Martin WR, Wieler M, Gee M (2008) Midbrain iron content in early Parkinson disease: a potential biomarker of disease status. Neurology 70 (16 Pt 2):1411–1417. [PubMed: 18172063]
11. Peran P, Cherubini A, Assogna F, Piras F, Quattrocchi C, Peppe A, Celsis P, Rascol O, Demonet JF, Stefani A, Pierantozzi M, Pontieri FE, Caltagirone C, Spalletta G, Sabatini U (2010) Magnetic resonance imaging markers of Parkinson's disease nigrostriatal signature. Brain 133 (11):3423–3433. [PubMed: 20736190]
12. Wallis LI, Paley MN, Graham JM, Grunewald RA, Wignall EL, Joy HM, Griffiths PD (2008) MRI assessment of basal ganglia iron deposition in Parkinson's disease. J Magn Reson Imaging 28 (5): 1061–1067. [PubMed: 18972346]
13. Aquino D, Contarino V, Albanese A, Minati L, Farina L, Grisoli M, Elia A, Bruzzone MG, Chiapparini L (2014) Substantia nigra in Parkinson's disease: a multimodal MRI comparison between early and advanced stages of the disease. Neurol Sci 35 (5):753–758. [PubMed: 24337946]
14. Focke NK, Helms G, Pantel PM, Scheewe S, Knauth M, Bachmann CG, Ebentheuer J, Dechent P, Paulus W, Trenkwalder C (2011) Differentiation of typical and atypical Parkinson syndromes by quantitative MR imaging. AJNR Am J Neuroradiol 32 (11):2087–2092. [PubMed: 21998102]
15. Isaias IU, Trujillo P, Summers P, Marotta G, Mainardi L, Pezzoli G, Zecca L, Costa A (2016) Neuromelanin Imaging and Dopaminergic Loss in Parkinson's Disease. Front Aging Neurosci 8:196. [PubMed: 27597825]
16. Mondino F, Filippi P, Magliola U, Duca S (2002) Magnetic resonance relaxometry in Parkinson's disease. Neurol Sci 23 Suppl 2:S87–88. [PubMed: 12548357]

17. Vymazal J, Righini A, Brooks RA, Canesi M, Mariani C, Leonardi M, Pezzoli G (1999) T1 and T2 in the brain of healthy subjects, patients with Parkinson disease, and patients with multiple system atrophy: relation to iron content. Radiology 211 (2):489–495. [PubMed: 10228533]

18. Ordidge RJ, Gorell JM, Deniau JC, Knight RA, Helpern JA (1994) Assessment of relative brain iron concentrations using T2-weighted and T2*-weighted MRI at 3 Tesla. Magn Reson Med 32 (3):335–341. [PubMed: 7984066]

19. Heim B, Krismer F, De Marzi R, Seppi K (2017) Magnetic resonance imaging for the diagnosis of Parkinson's disease. J Neural Transm (Vienna) 124 (8):915–964. [PubMed: 28378231]

20. Lehericy S, Vaillancourt DE, Seppi K, Monchi O, Rektorova I, Antonini A, McKeown MJ, Masellis M, Berg D, Rowe JB, Lewis SJG, Williams-Gray CH, Tessitore A, Siebner HR, International P, Movement Disorder Society -Neuroimaging Study G (2017) The role of high-field magnetic resonance imaging in parkinsonian disorders: Pushing the boundaries forward. Mov Disord 32 (4):510–525. [PubMed: 28370449]

21. Du G, Lewis MM, Sica C, He L, Connor JR, Kong L, Mailman RB, Huang X (2018) Distinct progression pattern of susceptibility MRI in the substantia nigra of Parkinson's patients. Mov Disord.

22. Ryvlin P, Broussolle E, Piollet H, Viallet F, Khalfallah Y, Chazot G (1995) Magnetic resonance imaging evidence of decreased putamenal iron content in idiopathic Parkinson's disease. Arch Neurol 52 (6):583–588. [PubMed: 7763206]

23. Sulzer D, Cassidy C, Horga G, Kang UJ, Fahn S, Casella L, Pezzoli G, Langley J, Hu XP, Zucca FA, Isaias IU, Zecca L (2018) Neuromelanin detection by magnetic resonance imaging (MRI) and its promise as a biomarker for Parkinson's disease. NPJ Parkinsons Dis 4:11. [PubMed: 29644335]

24. Nakane T, Nihashi T, Kawai H, Naganawa S (2008) Visualization of neuromelanin in the Substantia nigra and locus ceruleus at 1.5T using a 3D-gradient echo sequence with magnetization transfer contrast. Magn Reson Med Sci 7 (4):205–210. [PubMed: 19110515]

25. Sasaki M, Shibata E, Tohyama K, Takahashi J, Otsuka K, Tsuchiya K, Takahashi S, Ehara S, Terayama Y, Sakai A (2006) Neuromelanin magnetic resonance imaging of locus ceruleus and substantia nigra in Parkinson's disease. Neuroreport 17 (11):1215–1218. [PubMed: 16837857]

26. Schwarz ST, Rittman T, Gontu V, Morgan PS, Bajaj N, Auer DP (2011) T1-Weighted MRI shows stage-dependent substantia nigra signal loss in Parkinson's disease. Mov Disord 26 (9):1633–1638. [PubMed: 21491489]

27. Chen X, Huddleston DE, Langley J, Ahn S, Barnum CJ, Factor SA, Levey AI, Hu X (2014) Simultaneous imaging of locus coeruleus and substantia nigra with a quantitative neuromelanin MRI approach. Magn Reson Imaging 32 (10):1301–1306. [PubMed: 25086330]

28. Langley J, Huddleston DE, Chen X, Sedlacik J, Zachariah N, Hu X (2015) A multicontrast approach for comprehensive imaging of substantia nigra. NeuroImage 112:7–13. [PubMed: 25731994]

29. Hughes AJ, Daniel SE, Kilford L, Lees AJ (1992) Accuracy of clinical diagnosis of idiopathic Parkinson's disease: a clinico-pathological study of 100 cases. J Neurol Neurosurg Psychiatry 55 (3):181–184. [PubMed: 1564476]

30. Berardelli A, Wenning GK, Antonini A, Berg D, Bloem BR, Bonifati V, Brooks D, Burn DJ, Colosimo C, Fanciulli A, Ferreira J, Gasser T, Grandas F, Kanovsky P, Kostic V, Kulisevsky J, Oertel W, Poewe W, Reese JP, Relja M, Ruzicka E, Schrag A, Seppi K, Taba P, Vidailhet M (2013) EFNS/MDS-ES/ENS [corrected] recommendations for the diagnosis of Parkinson's disease. Eur J Neurol 20 (1):16–34. [PubMed: 23279440]

31. Langley J, Huddleston DE, Merritt M, Chen X, McMurray R, Silver M, Factor SA, Hu X (2016) Diffusion tensor imaging of the substantia nigra in Parkinson's disease revisited. Hum Brain Mapp 37 (7):2547–2556. [PubMed: 27029026]

32. Langley J, Huddleston DE, Sedlacik J, Boelmans K, Hu XP (2017) Parkinson's disease-related increase of T2*-weighted hypointensity in substantia nigra pars compacta. Mov Disord 32 (3): 441–449. [PubMed: 28004859]

33. Huddleston DE, Langley J, Dusek P, He N, Faraco CC, Crosson B, Factor S, Hu XP (2018) Imaging parkinsonian pathology in substantia nigra with MRI. Curr Radiol Rep 6:15.

34. Ulla M, Bonny JM, Ouchchane L, Rieu I, Claise B, Durif F (2013) Is R2* a new MRI biomarker for the progression of Parkinson's disease? A longitudinal follow-up. PLoS ONE 8 (3):e57904. [PubMed: 23469252]

35. Kitao S, Matsusue E, Fujii S, Miyoshi F, Kaminou T, Kato S, Ito H, Ogawa T (2013) Correlation between pathology and neuromelanin MR imaging in Parkinson's disease and dementia with Lewy bodies. Neuroradiology 55 (8):947–953. [PubMed: 23673875]

36. Usunoff KG, Itzev DE, Ovtscharoff WA, Marani E (2002) Neuromelanin in the human brain: a review and atlas of pigmented cells in the substantia nigra. Arch Physiol Biochem 110 (4):257–369. [PubMed: 12516659]

37. Huddleston DE, Langley J, Sedlacik J, Boelmans K, Factor SA, Hu XP (2017) In vivo detection of lateral-ventral tier nigral degeneration in Parkinson's disease. Hum Brain Mapp 38 (5):2627–2634. [PubMed: 28240402]

38. Ofori E, Pasternak O, Planetta PJ, Burciu R, Snyder A, Febo M, Golde TE, Okun MS, Vaillancourt DE (2015) Increased free water in the substantia nigra of Parkinson's disease: a single-site and multi-site study. Neurobiol Aging 36 (2):1097–1104. [PubMed: 25467638]

39. Burciu RG, Ofori E, Archer DB, Wu SS, Pasternak O, McFarland NR, Okun MS, Vaillancourt DE (2017) Progression marker of Parkinson's disease: a 4-year multi-site imaging study. Brain 140 (8):2183–2192. [PubMed: 28899020]

40. Ziegler DA, Wonderlick JS, Ashourian P, Hansen LA, Young JC, Murphy AJ, Koppuzha CK, Growdon JH, Corkin S (2013) Substantia nigra volume loss before basal forebrain degeneration in early Parkinson disease. JAMA Neurol 70 (2):241–247. [PubMed: 23183921]

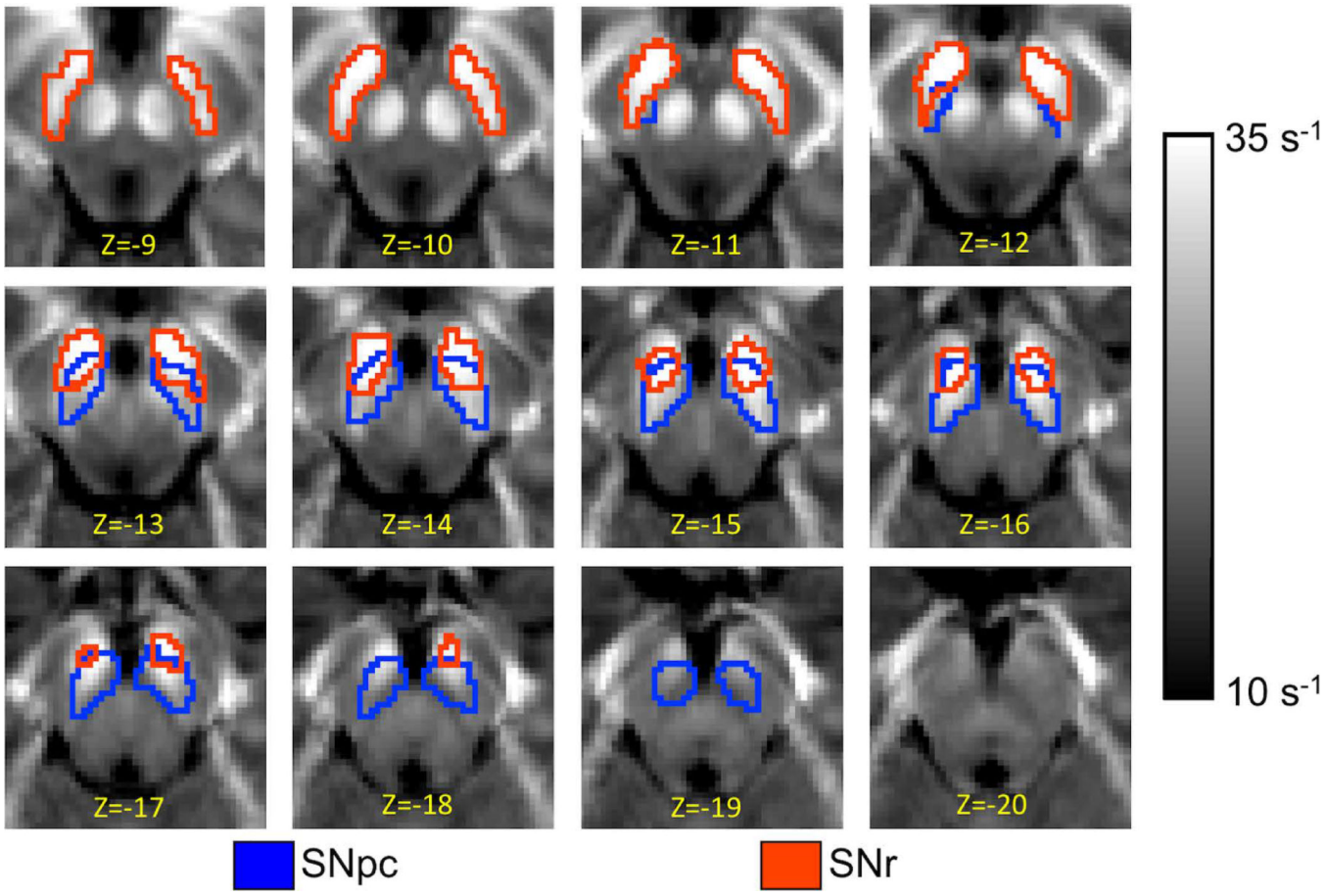

Figure 1.

A comparison of SNpc, outlined in blue, and SNr, and outlined in red, ROIs used in the multicohort analysis. The SNpc and SNr ROIs were derived from neuromelanin-sensitive and T_2*-weighted images, respectively. The ROIs are overlaid on the mean R_2* map derived from controls in cohort 1.

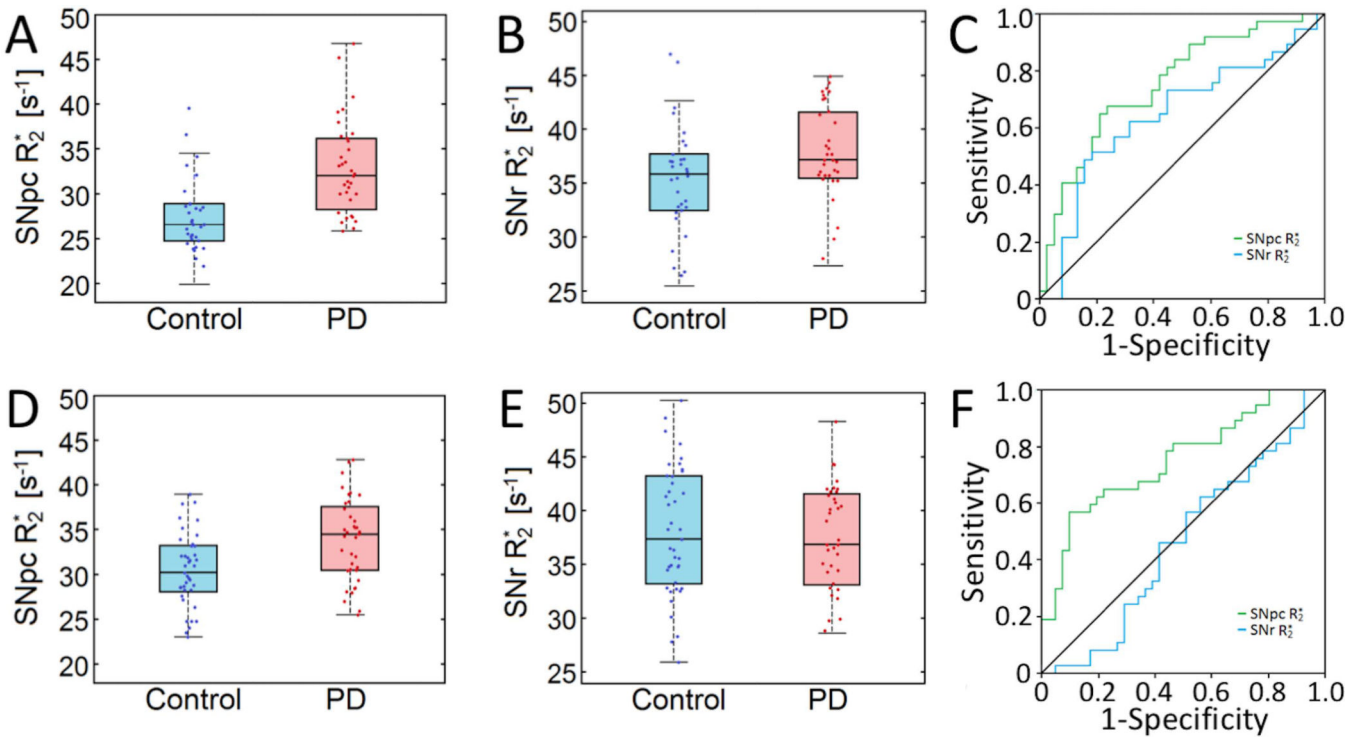

Figure 2.

Comparison of SNpc R_2* and SNr R_2* in cohort 1 (shown in A and B, respectively) and of SNpc R_2* and SNr R_2* in cohort 2 (shown in D and E, respectively). Statistically significant differences are seen in mean SNpc R_2* both cohorts. In A, B, D, and E, the box denotes the 25th and 75th percentile with the line denoting the median value. ROC analyses of nigral iron deposition are shown for cohort 1 in C and cohort 2 in F, respectively.

Table 1.

Demographic information and clinical characteristics of PD patients and healthy controls in cohorts 1 and 2. Data are presented as mean ± standard deviation unless otherwise noted.

Cohort 1				Cohort 2			
Variable	**HC (n=32)**	**PD (n=37)**	***p*Value**	**Variable**	**HC (n=46)**	**PD (n=42)**	***p*Value**
Gender (M/F)	12/20	19/18	0.26	Gender (M/F)	21/25	17/25	0.63
Age (yrs)	63.0±9.0	64.5±9.2	0.51	Age (yrs)	63.1±7.2	63.6±7.0	0.74
Education (yrs)	16.7±2.5	16.0±2.6	0.25	Education (yrs)	10.7±3.3	12.0±3.8	0.09
MOCA score	27.7±2.4	28.0±1.8	0.61	MMSE score	28.4±1.2	28.6±1.2	0.42
UPDRS-III score	2.2±3.1	19.8±5.9	2.2×10^{-23}	UPDRS-III score	—	22.2±12.4	—
Disease Duration (yrs)	—	4.3±4.1	—	Disease Duration (yrs)	—	6.1±4.6	—